D region electron density derived from sprite observations

Hans C. Stenbaek-Nielsen[1], Ningyu Liu[2], Matthew G McHarg[3], and Jacob Harley[3]

[1]University of Alaska Fairbanks
[2]The University of New Hampshire
[3]US Air Force Academy

November 26, 2022

Abstract

Four upward propagating streamers in 2 carrot sprites over northwest Texas were recorded at 100,000 frames per second at 07:46:35 UT, 2 June 2019, from the New Mexico Tech Langmuir Laboratory near Socorro, New Mexico. The streamers reached velocities of 50-80$\times 10^6$ m/s with accelerations up to 25×10^{10} m/s/s. The upward motion ended with the top of the streamers near 90 km altitude. At this time the streamers reached maximum brightness. The streamer head then dissolved and the brightness decayed exponentially with time constants between 0.078 and 0.097 ms. We interpret the dissolution and decay to be the result of interaction with the bottom of the ionosphere. Assuming the decay to be dictated by electric field relaxation, the ambient D region electron density may be derived. The analysis suggests that sprite observations can provide multipoint measurements of the D region ionosphere impacted by powerful lightning capable of triggering sprites.

Hosted file

`essoar.10512548.1.docx` available at https://authorea.com/users/533079/articles/605670-d-region-electron-density-derived-from-sprite-observations

D region electron density derived from sprite observations

H. C. Stenbaek-Nielsen[1], N. Y. Liu[2], M. G. McHarg[3], J. Harley[3]

[1]Geophysical Institute, University of Alaska Fairbanks, Fairbanks, Alaska 99775, USA

[2]Department of Physics and Astronomy, University of New Hampshire, Durham, New Hampshire 03824, USA

[3]Department of Physics and Meteorology, United States Air Force Academy, Colorado Springs, Colorado 80840, USA

Corresponding author: H. C, Stenbaek-Nielsen (hcnielsen@alaska.edu)

Key Points:

- Upward propagating streamers in sprites were recorded at 100,000 frames per second
- The streamer head decay is exponential; assuming it is due to electric field relaxation the ambient D region electron density can be derived
- Analysis suggests that sprites can provide multipoint measurements of D region impact by powerful lightning capable of triggering sprites

Abstract

Four upward propagating streamers in 2 carrot sprites over northwest Texas were recorded at 100,000 frames per second at 07:46:35 UT, 2 June 2019, from the New Mexico Tech Langmuir Laboratory near Socorro, New Mexico. The streamers reached velocities of 50-80$\times 10^6$ m/s with accelerations up to 25$\times 10^{10}$ m/s/s. The upward motion ended with the top of the streamers near 90 km altitude. At this time the streamers reached maximum brightness. The streamer head then dissolved and the brightness decayed exponentially with time constants between 0.078 and 0.097 ms. We interpret the dissolution and decay to be the result of interaction with the bottom of the ionosphere. Assuming the decay to be dictated by electric field relaxation, the ambient D region electron density may be derived. The analysis suggests that sprite observations can provide multipoint measurements of the D region ionosphere impacted by powerful lightning capable of triggering sprites.

Plain Language Summary

Sprites have been recorded at 100,000 frames per second. Analysis of the decay of upward propagating streamers indicates that the observations may be used to infer the ambient electron densities in the D region ionosphere impacted by powerful lightning capable of triggering sprites.

1 Introduction

Sprites are highly structured electrical discharges in the mesosphere/lower ionosphere driven by the quasi-electrostatic field (QE) from powerful cloud-

to-ground lightning (CG) strikes (Pasko, 2010; Stenbaek-Nielsen et al., 2013; Liu et al., 2015). They are predominantly caused by positive CG, with its QE field in the upper atmosphere pointing downward. In still images, a fully developed sprite displays a structured main body with a diffuse top (e.g., Pasko & Stenbaek-Nielsen, 2002). The filamentary structures of sprites are the manifestation of their building blocks: Streamer discharges (e.g. Cummer et al., 2006; Stenbaek-Nielsen et al., 2013; Liu et al., 2015). High speed observations indicate that sprites caused by +CGs are initiated by downward positive streamers, and upward negative streamers may start later from existing structures/channels resulting from the positive streamers (McHarg et al., 2007).

The propagation characteristics of positive sprite streamers have been investigated by past observational studies. It has been established that a positive streamer accelerates, expands, brightens and frequently branches, as it propagates downward, in excellent agreement with modeling results (Liu et al., 2009). A streamer is an ionization wave driven by a strongly enhanced electric field in its head. The field in the streamer head greatly exceeds the conventional breakdown threshold field, rapidly increasing the ionization density there via electron impact ionization to extend the streamer plasma channel forward. As negative sprite streamers propagate upward, they eventually encounter an increasing electron number density in the ionosphere. This affects the propagation and it may be possible to extract the information about the D region ionosphere, particularly the state after the early ionospheric response to the powerful lightning causing the upward negative streamer.

In this paper we present a sprite event recorded at 100,000 frames per second with two carrots, each of which has two well-defined upward propagating streamers. We show the 4 upward streamers as they brighten during the upward propagation, transit from discrete to a more diffuse appearance and the upward propagation stops, and finally, their rapid exponential decay. Assuming the observed decay to be due to electric field relaxation we can derive the ambient electron density at the altitude of the streamer. With several upward streamers over a limited horizontal area (a few tens of km), the analysis method may provide a unique opportunity for multipoint measurements to show how the D region ionosphere is impacted by powerful lightning capable of triggering sprites.

2 Instrumentation

The sprite high-speed images were recorded with an intensified Phantom V2611 camera. The intensifier is a VS-1845HS with extended blue sensitivity and a P46 phosphor (1 µs decay) preventing persistence onto following images. The Phantom V2611 camera has a 1280x800 pixel format CMOS and the images are 12 bits (4096 gray levels). However, at 100,000 fps hardware limitations reduce the usable image size. For the event reported here the image size is 512x320 pixels. The front lens was an 85 mm Nikon f/1.4, resulting in a field of view of 9.92x6.26 degrees. At a range of 690 km the pixel size is 242 m. The Phantom camera uses GPS time, and it is controlled by a laptop computer which

also is also used for the storage of events initially recorded in camera memory. Co-mounted with the Phantom camera we had a low light-level video camera (Watec 902H) to provide scene awareness and to record the star background critical for accurate pointing information.

3 Data and Analysis

The event, with two sprite carrots, was recorded at 100,000 frames per second on June 2, 2019, at 07:46:35 UT from the mountain top Langmuir Laboratory west of Socorro, NM, at 34.06N, 106.90W at an altitude of 3.3 km. A video of the event can be found at OSF project "D region electron density derived from sprites", https://doi.org/10.17605/OSF.IO/7WQTC. The event is 1 of 63 sprites recorded on the nights of 2 and 3 June, 2019, over a very active thunderstorm complex in north-west Texas (Figure 1, bottom panel). An analysis of the 63 sprites and their relation to sprite currents has been presented by Contreras-Vidal et al (2021). The 2 carrots are relatively weak compared to most of the 63 sprites, and Contreras-Vidal et al., extracted no sprite currents for the event.

Figure 1, top left, is an integration of images from the Phantom video to show the general morphology of the two sprite carrots. They are both 'classical' carrots. The luminosity along the central axes is from the initial downward streamer, and to the left and right we have the upward propagating streamers. Figure 1 right has the same image with the image sections, the tall rectangular boxes, used to show the temporal development of the upward streamers (Figure 2) as they propagate up, transit from discrete to diffuse, and then fade. The small rectangular boxes show the image section used to analyze the fade of the streamer head (Figure 3). The bottom of Figure 1 has a GOES map showing the storm complex associated with the event. Note the very cold cloudtop temperatures.

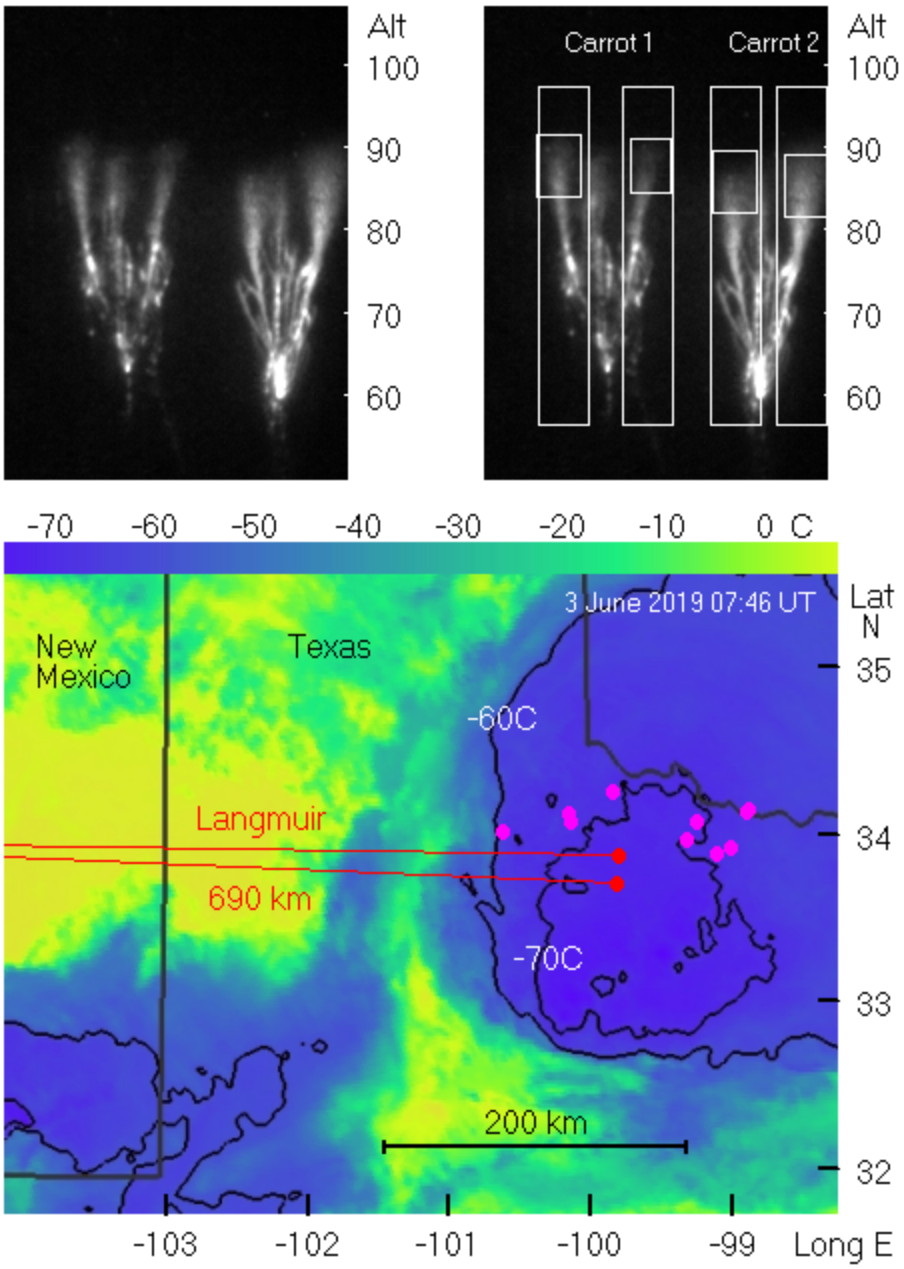

Figure 1. Upper Left: Time integrated image showing the 2 carrot sprites as observed from Langmuir Laboratory, NM, at 07:46:35 UT on 2 June 2019. The recording was at 100,000 frames per second. Upper Right: Same image with the sections (large rectangles) used to show the spatial development of the 4

upward streamers (Figure 2 below), and the sections (small rectangles) used to analyze the temporal development of the streamer brightness (Figure 3 below). The bottom panel is a GOES IR map with cloud top temperatures of the storm complex over which the carrots occurred. The assumed locations of the carrots are the red dots, and the magenta dots are lightning strikes associated with sprites observed within 1 hour of 07:46:35 UT.

The observations are from 1 station only so their geographic location cannot be determined by triangulation. In this case we customarily use the range to the causal lightning strike to determine the location, but unfortunately, we do not have any cloud to ground strikes for the event. Data from the Earth Networks Total Lightning Network (ENTLN) have several large intra-cloud flashes in the direction to and at the time of the sprite. They are at a range of 690 km from Langmuir and we will use this range for analysis. The 690 km range locates the carrots over the coldest cloud top temperatures on the GOES map (Figure 1). The 2 carrot locations are shown by the red dots on the map together with strikes (in magenta) leading to sprites within 1 hour of 04:46:35 UT. The range defines the image pixel size to 242 m.

Sprites are rarely right above the causal strike. This introduces a significant uncertainty on altitude. Sao Sabbas et al. (2003) found a median distance of 40 km in an analysis of 40 triangulated sprites. A 40 km uncertainty on the streamer data presented here translates in to a +-5 km uncertainty on altitude. There are many published triangulated sprites which provide an expected altitude range for various sprite features, and against these data the altitude scale derived using the 690 km range is quite reasonable. A recent discussion of sprite location relative to the causal lightning strike has been given by Stenbaek-Nielsen et al. (2020).

The temporal development of the two carrots is very similar. The onset of Carrot 1(left in figure 1) is a downward streamer with onset around 07:46:35.1534 UT at an altitude of 85 km. The onset of Carrot 2 (right in figure 1) is around 07:46:35.1652 UT at 79 km. In both carrots no halo emissions were observed and the initial single downward streamer appeared out of a dark background sky which makes the onset times very difficult to pin point. This is particularly the case for Carrot 1 where the determination of the onset time was helped by diffuse emissions above streamer onset. We often see these emissions in our high speed images (McHarg et al., 2007; Stenbaek-Nielsen et al., 2007; Stenbaek-Nielsen and McHarg, 2008) and their association with the downward streamers have been verified in simulations by Kosar et al. (2012). Only 5.50 ms after the onset time given above would the streamer become bright enough to be consistently present in successive frames. At that time the streamer had descended to an altitude of 74.4 km. For Carrot 2 the corresponding values are 0.47 ms and 78.5 km. The total length of optical emissions is 29.6 ms for Carrot 1 and 11.8 ms for Carrot 2. We note that the 4 upward streamers in the 2 carrots all appear over a period of only 6 ms as shown in the accompanying video.

Both carrots have two well-defined upward streamers to the left and right side

of the central axis defined by the initial downward streamer. Critical to the analys is that the streamers appear against a largely dark background allowing for analysis without interference from other luminous sprite structures. The onsets of the upward propagating streamers are all in the top of lower altitude glow from the initial downward streamer, as has been reported for other sprites (McHarg et al., 2007; Li & Cummer, 2011). For Carrot 1, the left carrot in Figure 1 (top), the onset altitudes are 69.3 km and 69.5 km for the left and right streamer, respectively, and 66.7 km for both right and left streamer in Carrot 2. The onset times for the left and right streamers in Carrot 1 are 11.0 ms and 11.1 ms, respectively, from the onset of the initial downward propagating streamer. For Carrot 2 the left and right streamer onset times are 3.9 ms and 3.6 ms after the initial downward streamer.

The 4 upward streamers propagate with increasing velocity and brightness reaching a maximum altitude of about 90 km. At or near this time the brightness integrated over the entire streamer head also reaches a maximum. After that they fade very rapidly. Figure 2 shows image time series for the 4 upward propagating streamers centered on the maximum brightness frame. The image strip time series cover 0.70 ms of time (70 phantom images). The individual image strips extracted from the Phantom images are defined by the tall rectangular boxes in Figure 1 (top right). The size of the box evaluated at the distance of the carrots is 6x41 km. To provide a reasonable spatial resolution strips are shown for every third image only, and to better show fainter features the intensity has been scaled by the square root of the intensity in the original images. The time shown at the bottom of the figure is ms from the onset of the upward propagating streamer.

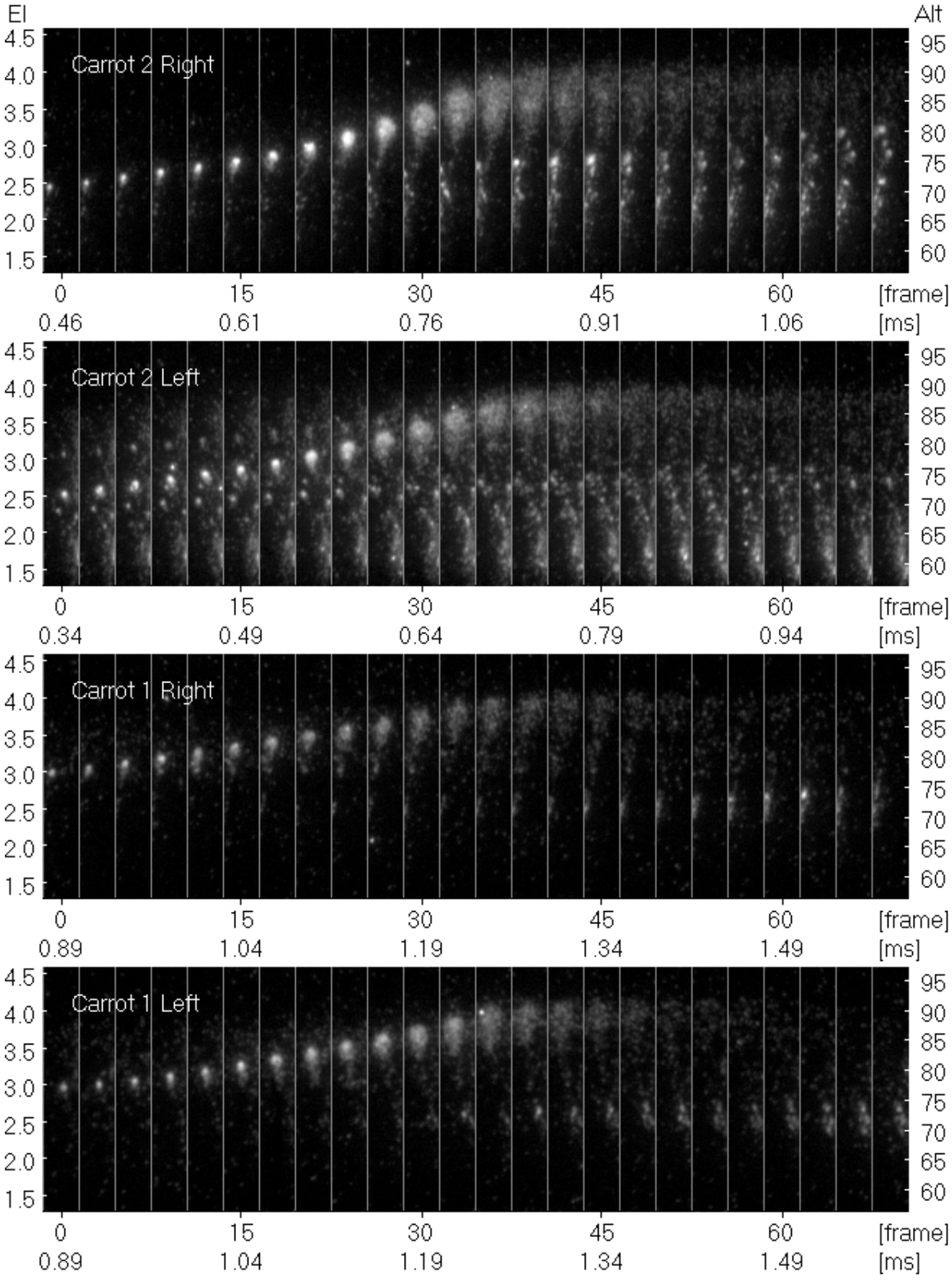
El
Alt
Carrot 2 Right
Carrot 2 Left
Carrot 1 Right
Carrot 1 Left
4.5
4.0
3.5
3.0
2.5
2.0
1.5
95
90
85
80
75
70
65
60
0
15
30
45
60
[frame]
0.46
0.61
0.76
0.91
1.06
[ms]
0.34
0.49
0.64
0.79
0.94
0.89
1.04
1.19
1.34
1.49

Figure 2. Image strip time series showing the brightening and decay of the 4 upward propagating streamers. The time series are centered on the start of the decay, frame 35. The sections of the Phantom images extracted for each streamer are show in Figure 1 top right. Each time series shows image strips for every third Phantom images and covers 0.70 ms of time. The intensities have been scaled by the square root to better show fainter features. The altitude scale is derived assuming a range of 690 km. The ms time scale for each series is from onset of the upward streamer. The onsets for Carrot 1 Left and Right differ by 0.08 ms, but the time to the start of the decay is the same.

The left half of the 4 image time series, frames 0 to 35, covers the upward moving and brightening streamer. Note that at an altitude near 80 km the streamer head transits from a well defined small bright head to a larger more diffuse structure. This is likely due to the rapidly increasing volume around the streamer head with E-fields large enough to generate optical emissions. The right half, frame 35 to 69, covers the rapid decay of the streamer. The best optical images are from the right upward streamer in Carrot 2 (near the right edge of the image in Figure 1), and we show that at the top of the figure followed by Carrot 2 Left, Carrot 1 Right, and at the bottom, Carrot 1 Left.

The brightness and upward velocity of the upward propagating streamers are initially low, but increase steadily as the streamers propagate upwards. At the times covered in Figure 2 the inferred velocities are among the highest we have observed. The highest velocity we have seen is 140×10^6 m/s, almost half the speed of light; it was reported by McHarg et al. (2002), using a 10 kHz photometer array. For the carrot in the top panel of Figure 2 (Carrot 2 Right) we infer a maximum upward velocity of 76×10^6 m/s. The high velocities are over a few frames only, so given the very dynamic nature of the events, the high values are partly a consequence of the large framing rate, 100,000 fps. Velocities inferred for the other 3 upward streamers are similar, but smaller.

If the acceleration is constant the altitude versus time would fit a parabola. For the Carrot 2 Right upward streamer, top panel in Figure 2, a fit shortly after onset indicates an acceleration of 2×10^{10} m/s/s increasing to 25×10^{10} m/s/s in a fit between 0.65 and 0.75 ms in Figure 2 (11 images in the recording). 25×10^{10} m/s/s is higher than previously reported. Li and Cummer (2009) give a maximum downward acceleration of 10^{10} m/s/s. McHarg et al. (2007) report an average upward acceleration of 1.8×10^{10} m/s/s, and note agreement with the theoretical predictions by Liu and Pasko (2004).

The top of the 4 upward propagating streamers reach an altitude near 90 km. At this time the streamers are also at their maximum integrated brightness. In the images the maximum altitude for Carrot 1 appears to be about 2 km higher than the maximum altitude observed in Carrot 2, but this may not be real. The altitude of each streamer is determined assuming a range of 690 km, but both carrots may not be at that range. The higher altitudes may simply be from the left carrot being closer to the observer and therefore will appear higher in the sky. If we assume the tops to be at the same altitude Carrot 1 would be 13 km

closer to the observer than Carrot 2.

The streamer brightness increases steadily towards a maximum near the time of maximum altitude and decays rapidly thereafter, as shown in Figure 3. The time covered is the same as for Figure 2. The individual points were derived by summing over the image pixels covering the streamer head. Initially the image section with the streamer is set frame by frame, but after the brightness peak the altitude does not change, and we then use a fixed image section. The locations of the fixed image section for each streamer are the small rectangles shown in Figure 1 top right. The sampling area and the altitude range covered vary between the 4 streamers, but is about 5x7 km and located between 82 and 90 km.

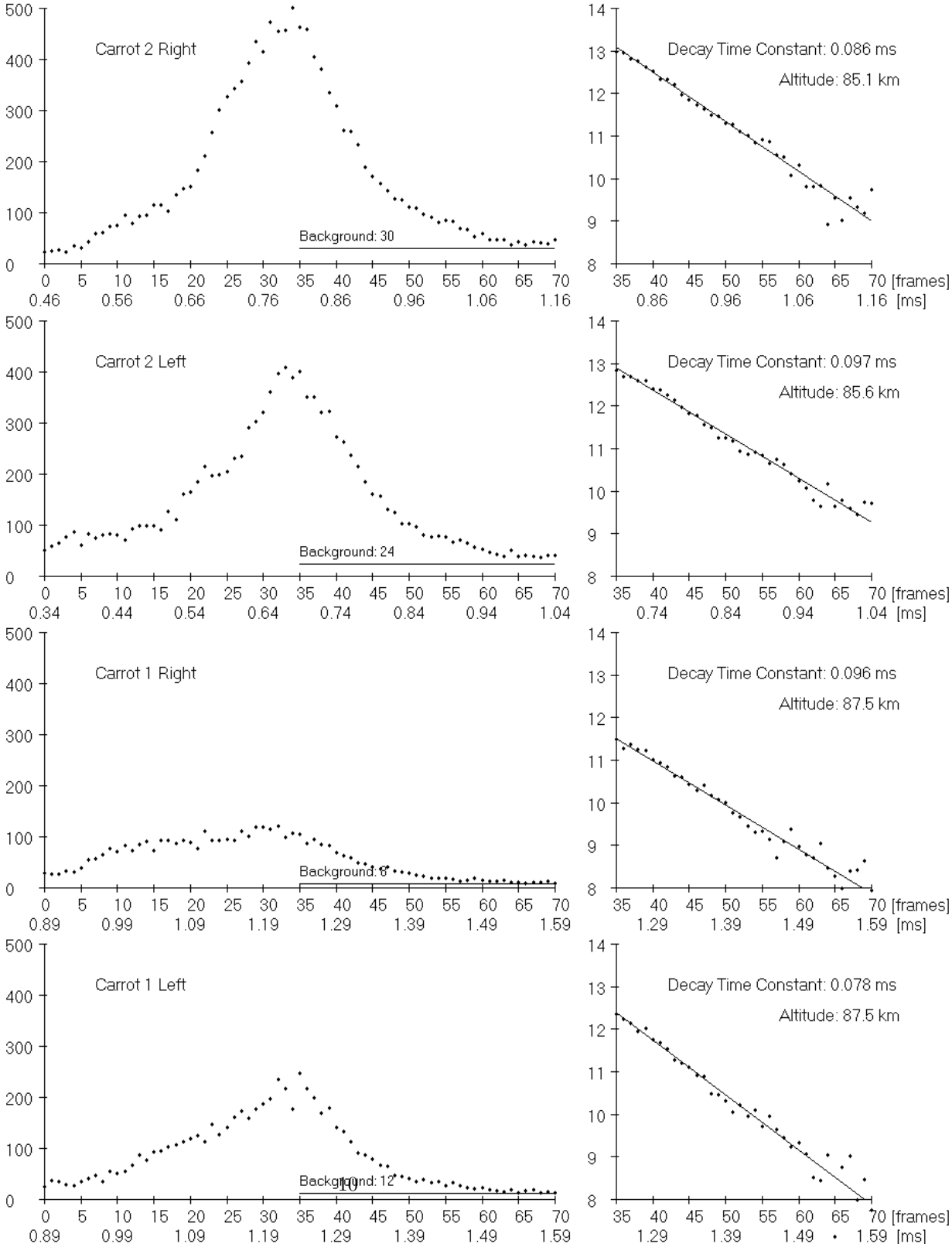
Carrot 2 Right
Background: 30
Decay Time Constant: 0.086 ms
Altitude: 85.1 km
Carrot 2 Left
Background: 24
Decay Time Constant: 0.097 ms
Altitude: 85.6 km
Carrot 1 Right
Background: 8
Decay Time Constant: 0.096 ms
Altitude: 87.5 km
Carrot 1 Left
Background: 12
Decay Time Constant: 0.078 ms
Altitude: 87.5 km
[frames]
[ms]

Figure 3. Streamer brightness derived by summing pixel values over the streamer area in 70 consecutive images. The time covered is the same as in Figure 2. The brightness sequences are centered on image 35 where the streamer decay starts. The left plot has the brightness plotted on a linear scale; on the right the brightness, less a background brightness value, is plotted on a (natural) logarithmic scale to show exponential decay. The background brightness value is given on the linear plot, and the inferred decay time constant and altitude is given on the logarithmic plot. The ms time axis for the 4 streamers are from the onset of the upward streamer.

Except for Carrot 2 Right the streamers do not saturate the imager and the brightness is simply a sum of pixel values over the area in the image of the streamer. In Carrot 2 Right there are saturated pixels in images between images 16 and 27. The streamer brightness profile often fits a Gaussian very well (Stenbaek-Nielsen et al., 2007), and we used that to compensate for the undercount resulting from saturated pixels. In the affected images the number of saturated pixels is relatively small and the correction to individual points in Figure 3 is generally only a few % and at most 10 %. Note that the images with saturated pixels are before the peak brightness at image 35.

The decay of the streamer is very rapid starting at image 35. The decay is clearly exponential as shown in the right section of Figure 3 in which the brightness less an assumed background brightness is plotted on a natural logarithmic scale. The background level was initially set for each streamer by visually estimating the value of an asymptotic decay and then refined by minimizing the sum of the error on the linear display. The decay time constant and streamer head attitude for the 4 upward propagating streamers are in the order displayed on Figures 2 and 3: 0.086 ms at 85 km; 0.097 ms at 86 km; 0.096 ms at 88 km; and 0.078 ms at 88 km respectively. These values are also on the figure. The uncertainty on the time constants is estimated at 5 %, so the differences in the decay time constant between the 4 streamers are statistically significant.

To look for altitude dependence in the derived decay time constants we did a similar analysis for each streamer using smaller areas at different altitudes. The variations in the derived decay time constants were small and there were no consistent altitude trends. Therefore, no indication was found for an altitude dependence of the decay time constant within each of the 4 streamers.

4 Discussion

The observations of sprite streamers at 100,000 fps have revealed accelerations up to 25×10^{10} m/s/s, which is higher than previously reported in the literature. The observed high accelerations do not last long and are in part attributable to the high time resolution. The upward propagating streamers stop at altitudes near 90 km after which the luminosity decays exponentially. The decay time constants in the 4 streamers analyzed are fairly similar ranging from 0.078 ms to 0.097 ms (Figure 3), but the range exceeds the estimated 5 % uncertainty and therefore indicates real differences in the decay.

We assume that the decay is a consequence of the streamers interacting with the lower ionosphere where the electron density, and therefore conductivity, increases rapidly with altitude. When the streamer enters the higher conductivity region it will lose charge faster than the current in the streamer channel, driven by the propagating streamer head, can supply, and the streamer head will rapidly dissolve.

The optical emissions from the streamers are dominated by the $1PN_2$ band (Liu & Pasko, 2004; Stenbaek-Nielsen et al., 2020). Ignoring contributions from higher-energy states, the number, n, of exited molecules leading to the emissions is governed by (Liu & Pasko, 2004):

$dn/dt + n/ \quad = \quad n_e$, (1)

where is the lifetime of the excited state, is the excitation frequency, and n_e is electron density. The term n_e is the rate of excitation (source term) and n/ is the rate of de-excitation through emission or quenching (loss term). Because the altitude of interest (~85 km) is much higher than the quenching altitude of 53 km for $1PN_2$, is equal to the natural lifetime (1/A) of 5.9 µs for $1PN_2$, where $A = 1.7 \times 10^5$ s^{-1} is the radiation transition rate (Vallance Jones,1974). The product An gives the emission rate (s^{-1} m^{-3}). The observed decay of the streamer head has a time constant much longer than , and therefore, the forcing term n_e on the right-hand side must decay with the observed time constant.

Because is proportional to the electric field, and the lifetime of n_e is much longer than 100 µs at ~85 km altitude (e.g., Sentman et al., 2008), the decay of the forcing term signals that the electric field decreases, which is presumably due to electric field relaxation. The electric field relaxation time is $_E = _0/ = _0/(e\mu_e n_e)$, where $_0$ is the permittivity of free space, $= e\mu_e n_e$ is conductivity, e is the elementary charge, μ_e is electron mobility, and n_e is electron density. If we simply take the optical decay time constant, $_o$, as the electric field relaxation time, the electron density can be estimated as $n_e = _0 / (e\ \mu_e\ _o)$. Note μ_e is a function of both electric field and neutral density (Liu & Pasko, 2004). The observed decay time constant and average streamer head altitude for the 4 upward propagating streamers are: 0.086 ms at 85 km; 0.097 ms at 86 km; 0.096 ms at 88 km; and 0.078 ms at 88 km respectively. Assuming an electric field of 0.5-1.5E_k, a reasonable range for sprites, the estimated electron densities, in the same order as on figures 2 and 3, are: 7.7-9.7×10^7 m^{-3}; 5.6-7.3×10^7 m^{-3}; 3.9-5.1×10^7 m^{-3}; and 4.8-6.3×10^7 m^{-3}. Those values are about two orders of magnitude smaller than the electron density in a streamer channel at 85 km. Our interpretation is that they represent the ambient electron density at the altitude of the streamer head.

Additional insight can be obtained by considering a one-dimensional model of the continuity equation that governs electric field dynamics (equation (7) in Kosar et al., 2012). Because the electric field relaxation time corresponding to the streamer channel conductivity at the altitude of interests is of the order of only 0.02 ms, the decay of the field, ~0.100 ms, must be due to a decaying

total current with the same timescale. Because the total current is altitude independent, this explains why the observed optical decay constant has no strong dependence on the altitude.

The derived electron densities compare reasonably well with published data. Liu (2012) found 5×10^7 m^{-3} in a halo simulation, and later 3×10^7 m^{-3} in a negative sprite simulation (Liu et al., 2016). Han and Cummer (2010) inferred from an analysis of VLF observations a density of 3×10^7 m^{-3} at ~85 km altitude. VLF observations can provide information on the variability of the D region ionosphere (Lay & Shao, 2011; Gross & Cohen, 2020; Golkowski et al., 2021) with horizontal spatial resolution of tens of kilometers. Using the sprite streamer decay rates to infer electron densities would have a spatial resolution of only a few km and can therefore refine the VLF data.

The Phantom recordings presented here are from 1 station only, resulting in significant uncertainty on sprite location and altitude, as explained above in the Data and Analysis section. To be able to accurately determine the streamer head location and altitude will require extra information. The obvious solution is to make multi-station optical observations, so that the streamer locations can be determined by triangulation. The additional observations need not be with high-speed cameras; a video camera or a digital camera will suffice. All that is needed is an image in which the direction to the sprite feature of interest can be determined and used for triangulation.

The 4 streamers in the analysis presented here have essentially the whole streamer appearing against a largely dark sky. They were the best examples in the 2019 high-speed sprite recordings. We do have similar good events in data from earlier years, but at much lower frame rates. An example was shown in Stenbaek-Nielsen et al. (2013) – their Figure 5 - recorded at 12,500 fps. At this framerate the decay is only in 3 frames which is insufficient for a good determination of the decay time constant. This emphasizes the need for significantly higher framerates.

The event selection criteria used in the analysis presented, with essentially the whole streamer appearing against a largely dark sky, is very restrictive. However, the decay time constant can be derived based on just a small area of the large diffuse streamer head and a sufficient number of frames to determine the decay rate. This is a much less stringent selection criterion. With upward streamers a very common feature in sprites the analysis presented here provides a method to remotely investigate the electron densities in the bottom of the ionosphere above sprite producing thunderstorms.

Acknowledgements

We thank Dr. H. Eden and colleagues at the Langmuir Laboratory, Socorro, NM, for their hospitality and support during the 2019 sprite observations, and MSgt Nathaniel C. George, USAFA, for assistance with the GOES map used in Figure 1. The GOES image was obtained from NOAA Comprehensive Large Array-data Stewardship System (CLASS). This research was partially supported under

DARPA Cooperative Agreement HR00112120003 via a subcontract with Embry-Riddle Aeronautical University, by the Air Force Office of Scientific Research. This work is approved for public release; distribution is unlimited. The content of the information does not necessarily reflect the position or the policy of the Government, and no official endorsement should be inferred.

Data Availability Statement

A 100,000 fps video of the streamers presented here is available at Open Science Framework (OSF) in project "D region electron density derived from sprites", https://doi.org/10.17605/OSF.IO/7WQTC.

References

Contreras-Vidal, L., Sonnenfeld, R. G., da Silva, C. L., McHarg, M. G., Jensen, D., Harley, J., et al. (2021). Relationship between sprite current and morphology. Journal of Geophysical Research: Space Physics, 126, e2020JA028930. https://doi.org/10.1029/2020JA028930

Cummer, S. A., N. Jaugey, J. Li, W. A. Lyons, T. E. Nelson, and E. A. Gerken (2006), Submillisecond imaging of sprite development and structure, Geophys. Res. Lett., 33, L04104, doi:10.1029/2005GL024969.

Golkowski, M., C. Renick, and M. B. Cohen (2021), Quantification of ionospheric perturbations from lightning using overlapping paths of VLF signal propagation, Journal of Geophysical Research: Space Physics, 126 (5), e28540, doi:10.1029/2020JA028540.

Gross, N. C., and M. B. Cohen (2020), VLF remote sensing of the D region ionosphere using neural networks, Journal of Geophysical Research: Space Physics, 125 (1), e27135, doi:10.1029/2019JA027135.

Han, F., & Cummer, S. A. (2010), Midlatitude nighttime D region ionosphere variability on hourly to monthly time scales, J. Geophys. Res., 115, A09323, doi:10.1029/2010JA015437.

Kosar, B. C., N. Liu, & H. K. Rassoul (2012), Luminosity and propagation characteristics of sprite streamers initiated from small ionospheric disturbances at subbreakdown conditions, J. Geophys. Res., 117, A08328, doi:10.1029/2012JA017632

Lay, E. H., & Shao, X.-M. (2011). High temporal and spatial-resolution detection of D-layer fluctuations by using time-domain lightning waveforms. J. Geophys. Res., 116 (A1), A01317. doi: 10.1029/2010JA016018

Li, J., and S. A. Cummer (2009), Measurement of sprite streamer acceleration and deceleration, Geophys. Res. Lett., 36, L10812, doi:10.1029/ 2009GL037581.

Li, J., and S. Cummer (2011), Estimation of electric charge in sprites from optical and radio observations, J. Geophys. Res., 116, A01301, doi:10.1029/2010JA015391.

Liu, N. Y. (2012). Multiple ion species fluid modeling of sprite halos and the role of electron detachment of O- in their dynamics, Journal of Geophysical Research, 117, A03308, doi:10.1029/2011JA017062

Liu, N., and V. P. Pasko (2004), Effects of photoionization on propagation and branching of positive and negative streamers in sprites,J. Geophys. Res.,109, A04301, doi:10.1029/2003JA010064

Liu, N. Y., Pasko, V. P., Adams, K., Stenbaek-Nielsen, H. C., & McHarg, M. (2009). Comparison of acceleration, expansion and brightness of sprite streamers obtained from modeling and high-speed video observations. J. Geophys. Res,114 . doi: 10.1029/2008JA013720

Liu, N. Y., McHarg, M. G., & Stenbaek-Nielsen, H. C. (2015). High-altitude electrical discharges associated with thunderstorms and lightning. J. Atmos. Solar. Terr. Phys. doi: 10.1016/j.jastp.2015.05.013

Liu, N. Y., Boggs, L. D. & Cummer, S. A. (2016), Observation-constrained modeling of the ionospheric impact of negative sprites, Geophysical Research Letters, 43, doi:10.1002/2016GL068256

McHarg, M. G., R. K. Haaland, D. Moudry, and H. C. Stenbaek-Nielsen (2002), Altitude-time development of sprites, J. Geophys. Res., 107(A11), 1364, doi:10.1029/2001JA000283.

McHarg, M. G., Stenbaek-Nielsen, H. C., & Kammae, T. (2007). Observation of streamer formation in sprites. *Geophysical Research Letters, 34*, L06804. https://doi.org/10.1029/2006GL027854

Pasko, V. P. (2010). Recent advances in theory of transient luminous events. J. Geophys. Res., 115 . doi: 10.1029/2009JA014860

Pasko, V. P., & Stenbaek-Nielsen, H. C. (2002). Diffuse and streamer regions of sprites. Geophys. Res. Lett., 29 (10). doi: 10.1029/2001GL014241

Sao Sabbas, F., Sentman, D., Wescott, E., Pinto Jr., O., Mendes Jr., O., & Taylor, M. (2003). Statistical analysis of space-time relationships between sprites and lightning. *Journal of Atmospheric and Solar-Terrestrial Physics*, *65*, 525–535. https://doi.org/10.1016/S1364-6826(02)00326-7

Sentman DD, Stenbaek-Nielsen HC, McHarg MG, Morrill J (2008) Plasma chemistry of sprite streamers. J Geophys Res 113:D11112. doi:10.1029/2007JD008941

Stenbaek-Nielsen, H. C., M. G. McHarg, T. Kanmae, and D. D. Sentman (2007), Observed emission rates in sprite streamer heads, *Geophys. Res. Lett., 34,* L11105, doi:10.1029/2007GL029881

Stenbaek-Nielsen, H. C., & McHarg, M. G. (2008). High time-resolution sprite imaging: Observations and implications. *Journal of Physics D: Applied Physics, 41,* 234009. https://doi.org/10.1088/0022-3727/41/23/234009

Stenbaek-Nielsen, H. C., Kanmae, T., McHarg, M. G., & Haaland, R. (2013). High-speed observations of sprite streamers. *Survey of Geophysics*, *34*, 769–795. https://doi.org/10.1007/s10712-013-9224-4

Stenbaek-Nielsen, H. C., McHarg, M. G., Haaland, R., & Luque, A. (2020). Optical spectra of small-scale sprite features observed at10,000 fps. Journal of Geophysical Research: Atmospheres, 125, e2020JD033170. https://doi.org/10.1029/2020JD033170

Vallance Jones, A. (1974). Aurora. D. Reidel, Dordrecht, Netherlands. https://doi.org/10.1007/978-94-010-2099-2